

# Supernova $\beta^-$ decay of nuclides $^{53}\text{Fe}$ , $^{54}\text{Fe}$ , $^{55}\text{Fe}$ and $^{56}\text{Fe}$ in strongly screened plasma

Jing-Jing Liu and Dong-Mei Liu

College of Electronic and Communication Engineering, Hainan Tropical Ocean University, Sanya 572022, China;  
[liujingjing68@126.com](mailto:liujingjing68@126.com)

Received 2017 August 22; accepted 2017 November 3

**Abstract** Electron screening has strong effects on electron energy and threshold energy of the beta decay reaction. In this paper, we study  $\beta^-$  decay rates of some iron isotopes. The beta decay rates increase by about two orders of magnitude due to electron screening. Strongly screened beta decay rates due to  $Q$ -value correction are more than one order of magnitude higher than those without  $Q$ -value correction.

**Key words:** physical data and processes: nuclear reactions, nucleosynthesis, abundances — stars: supernovae

## 1 INTRODUCTION

Beta decay plays a key role in presupernova evolution. The cooling rates and antineutrino energy loss are strongly affected by the beta-decay rates. Some authors (e.g., Fuller et al. 1982; Aufderheide et al. 1990, 1994; Langanke & Martinez-Pinedo 1998, Liu 2012, 2013e,d,f,c,a,b, 2014, 2015; Liu et al. 2016; Liu & Gu 2016; Gao et al., 2015, 2016, 2017a,b,c) conducted many studies on the beta decay and electron capture processes. However, the effect of strong electron screening (SES) on weak interaction has not been thoroughly investigated.

By applying the linear response theory model (LRTM) and shell model Fermi theory, we study SES beta decay rates of nuclides  $^{53}\text{Fe}$ ,  $^{54}\text{Fe}$ ,  $^{55}\text{Fe}$  and  $^{56}\text{Fe}$  in astrophysical environments, which are very important for numerical simulations of supernova explosions (e.g., Fuller et al. 1982; Aufderheide et al. 1990, 1993, 1994; Langanke et al. 2003; Domingo-Pardo et al. 2009). The article is organized as follows. In Section 2, we study beta-decay rates by including and neglecting the SES effect. In Section 3, the results and discussions are presented. The conclusions are given in Section 4.

## 2 STUDYING $\beta^-$ DECAY

### 2.1 Beta Decay with No SES

In the case of no SES, the  $\beta^-$  decay rates are given by (Fuller et al. 1982; Aufderheide et al. 1990, 1994; Liu

et al. 2016).

$$\lambda_{\text{bd}}^0 = \ln 2 \times \sum \frac{(2J_i + 1)e^{-\frac{E_i}{k_B T}}}{G(Z, A, T)} \times \sum_f \frac{\psi(\rho, T, Y_e, Q_{ij})}{ft_{ij}}, \quad (1)$$

where  $J_i$  is the spin and  $E_i$  is excitation energies of the parent states.  $k_B$  is the Boltzmann constant.  $ft_{ij}$  is the comparative half-life connecting states  $i$  and  $j$ , and  $Q_{ij}$  is the nuclear energy difference between the states  $i$  and  $j$ .  $Q_{00} = M_p c^2 - M_d c^2$ ,  $M_p$  and  $M_d$  are the masses of the parent nucleus and the daughter nucleus, respectively, and  $E_i$  and  $E_j$  are the excitation energies of the  $i$ th and  $j$ th nuclear state respectively.  $G(Z, A, T)$  is the nuclear partition function.

The phase space integral  $\psi(\rho, T, Y_e, Q_{ij})$  for the  $\beta^-$  decay is given by

$$\psi(\rho, T, Y_e, Q_{ij}) = \frac{c^3}{(m_e c^2)^5} \times \int_1^{Q_{ij}} \varepsilon_e (\varepsilon_e^2 - 1)^{1/2} (Q_{ij} - \varepsilon_e)^2 \times \frac{F(Z + 1, \varepsilon_e)}{1 + \exp[(U_F - \varepsilon_e)/k_B T]} d\varepsilon_e, \quad (2)$$

where  $p$ ,  $m_e$ ,  $U_F$  and  $\varepsilon_e$  are the electron momentum, mass, chemical potential and energy, respectively.  $F(Z + 1, \varepsilon_e)$  is the Coulomb wave correction.

In case no SES is present, a reasonable approximation for the electron chemical potential takes the form (e.g., Bludman & van Riper 1978)

$$U_F = 1.11(\rho_7 Y_e)^{1/3} \times \left[ 1 + \left( \frac{\pi}{1.11} \right) \frac{(k_B T)^2}{(\rho_7 Y_e)^{2/3}} \right]^{-1/3} \text{ MeV.} \quad (3)$$

According to discussions from Zhou et al. (2017), the half-life  $ft_{ij}$  can be expressed as

$$\begin{aligned} \ln(ft_{ij}) &= a_1 + (\alpha^2 Z^2 - 5 + a_2 \frac{N-Z}{A}) \\ &\quad \times \ln(Q_{if} - a_3 \delta) \\ &\quad + (a_4 \alpha^2 Z^2) + \frac{1}{3} \alpha^2 Z^2 \ln(A) \\ &\quad - \alpha Z \pi + S(N, Z), \end{aligned} \quad (4)$$

where  $\alpha$  is the fine structure constant with value  $1/137$ . The correction factor  $S(N, Z)$  can be written (e.g., Zhou et al. 2017)

$$\begin{aligned} S(N, Z) &= a_5 \exp(-((N-28)^2 + (N-20)^2)/12) \\ &\quad + a_6 \exp(-((N-50)^2 + (N-38)^2)/43) \\ &\quad + a_7 \exp(-((N-82)^2 + (N-50)^2)/13) \\ &\quad + a_8 \exp(-((N-82)^2 + (N-58)^2)/24) \\ &\quad + a_9 \exp(-((N-110)^2 + (N-70)^2)/244), \end{aligned} \quad (5)$$

where  $a_i (i = 1, 2, 3, \dots, 9) = 11.09, 1.07, -0.935, -5.398, 3.016, 3.879, 1.322, 6.030$  and  $1.669$  in Equations (4)-(5). In Equation (4), the shell and pairing effect on the nuclear matrix elements reflect the main information on nuclear structure. The factor  $\delta$  is well described by  $\delta = (-1)^N + (-1)^Z$  (Zhou et al. 2017).

The Fermi and Gamow-Teller (GT) matrix elements for  $\beta^-$  decay are given by (e.g., Aufderheide et al. 1994)

$$\begin{aligned} |M_F(fi)|^2 &= |\langle \omega_f^D | \sum_n (\tau_{\pm 1}) |\omega_i^P \rangle|^2 / (2J_i + 1) \\ &= |\langle j_p || (\tau_{\pm 1}) || j_n \rangle|^2 \frac{N_n}{(2j_n + 1)(2J_i + 1)} \\ &\quad \times \left( 1 - \frac{N_p}{2j_p + 1} \right), \end{aligned} \quad (6)$$

$$\begin{aligned} |M_{GT}(fi)|^2 &= |\langle \omega_f^D | \sum_n \sigma_n (\tau_{\pm 1}) |\omega_i^P \rangle|^2 / (2J_i + 1) \\ &= |\langle j_p || \sigma_n (\tau_{\pm 1}) || j_n \rangle|^2 \frac{N_n}{(2j_n + 1)(2J_i + 1)} \\ &\quad \left( 1 - \frac{N_p}{2j_p + 1} \right), \end{aligned} \quad (7)$$

where  $|\omega_i^P \rangle$  is the initial parent state and  $|\omega_f^D \rangle$  is the final daughter state.  $N_n$  and  $N_p$  are the numbers of neutrons and protons within the  $j_n$  and  $j_p$  shells, respectively.

The Shell Model Monte Carlo (SMMC) method is used to calculate the total amount of GT strength  $S_{GT-}$  and the response function  $R_A(\tau)$  of an operator  $\hat{A}$  at an imaginary time  $\tau$ .  $R_A(\tau)$  is given by (e.g., Langanke & Martinez-Pinedo 1998; Langanke et al. 2003)

$$R_A(\tau) = \frac{\sum_{if} (2J_i + 1) e^{-\beta E_i} e^{-\tau(E_f - E_i)} |\langle f | \hat{A} | i \rangle|^2}{\sum_i (2J_i + 1) e^{-\beta E_i}}, \quad (8)$$

where  $E_i$  and  $E_f$  are energies corresponding to the final states  $|i \rangle$  and  $|f \rangle$  respectively. The total strength for the operator is given by  $R(\tau = 0)$ . The strength distribution is given by

$$\begin{aligned} S_{GT+}(E) &= \frac{\sum_{if} \delta(E - E_f + E_i) (2J_i + 1) e^{-\beta E_i} |\langle f | \hat{A} | i \rangle|^2}{\sum_i (2J_i + 1) e^{-\beta E_i}} \\ &= S_A(E), \end{aligned} \quad (9)$$

which is related to  $R_A(\tau)$  by a Laplace Transform,  $R_A(\tau) = \int_{-\infty}^{\infty} S_A(E) e^{-\tau E} dE$ . Note that here  $E$  is the energy transfer within the parent nucleus, and that the strength distribution  $S_{GT+}(E)$  has units of  $\text{MeV}^{-1}$ , and  $\beta = 1/T_N$  and  $T_N$  is the nuclear temperature.

## 2.2 Beta Decay with SES

Electron screening for nuclear reactions in astrophysical environments plays an unexpected and important role in enhancing reaction cross sections. In our previous works (e.g., Liu 2013c, 2016; Liu et al. 2017a,b), we discussed this interesting problem. Based on LRTM, Itoh et al. (2002) also studied the influence of screening potential on the weak interaction. Electrons are strongly degenerate in our considerable regime of density and temperature, which is described as

$$T \ll T_F = 5.930 \times 10^9 \left\{ \left[ 1 + 1.018 \left( \frac{Z}{A} \right)^{2/3} (10\rho_7)^{2/3} \right]^{1/2} - 1 \right\}, \quad (10)$$

where the electron Fermi temperature and the density are  $T_F$  and  $\rho_7$  (in units of  $10^7 \text{ g cm}^{-3}$ ), respectively.

Jancovici (1962) studied the static longitudinal dielectric function for a relativistic degenerate electron liquid. The electron potential energy in SES is given by

$$V(r) = -\frac{Ze^2(2k_F)}{2k_F r} \frac{2}{\pi} \int_0^\infty \frac{\sin(2k_F r)q}{q\epsilon(q, 0)} dq, \quad (11)$$

where  $\epsilon(q, 0)$  is Jancovici's static longitudinal dielectric function and  $k_F$  is the electron Fermi wavenumber.

For relativistic degenerate electrons and based on LRTM, the screening potential is calculated as

$$D = 7.525 \times 10^{-3} Z \left( \frac{10z\rho_7}{A} \right)^{\frac{1}{3}} J(r_s, R) \text{ (MeV)}, \quad (12)$$

where the parameters  $J(r_s, R)$ ,  $r_s$  and  $R$  are discussed by Itoh et al. (2002) in detail. Equations (14) and (16) are satisfied for  $10^{-5} \leq r_s \leq 10^{-1}$ ,  $0 \leq R \leq 50$ , which is fulfilled in a presupernova environment.

When we account for the influence of SES, the beta decay  $Q$ -value changes by (Fuller et al. 1982)

$$\Delta Q \approx 2.940 \times 10^{-5} Z^{2/3} (\rho Y_e)^{1/3} \text{ MeV}. \quad (13)$$

Thus, the  $Q$ -value of beta decay changes from  $Q_{if}$  to  $Q'_{if} = Q_{if} - \Delta Q$ .

We cannot neglect its influence at high density when an electron is strongly screened due to the fact that the screening energy is so high. Electron screening makes electron energy increase from  $\varepsilon_e$  to  $\varepsilon_e^s = \varepsilon_e + D$  during beta decay. The screening also decreases the threshold energy from  $Q_{if}$  to  $Q_{if}^s(\text{I}) = Q_{if} + D$  and  $Q_{if}^s(\text{II}) = Q'_{if} + D = Q_{if} - \Delta Q + D$ , corresponding to SES models (I) and (II) respectively. SES models (I) and model (II) correspond to the case without and with correction by the  $Q$ -value respectively. So, the phase space integral  $\psi^s(\rho, T, Y_e, Q_{ij})$  replaces  $\psi(\rho, T, Y_e, Q_{ij})$  in Equation (2) for the SES beta decay rates, and is calculated as

$$\begin{aligned} \psi^s(\rho, T, Y_e, Q_{ij}^s) &= \frac{c^3}{(m_e c^2)^5} \int_{1+D}^{Q_{ij}^s} d\varepsilon_e^s \varepsilon_e^s \\ &\times \left[ (\varepsilon_e^s)^2 - 1 \right]^{1/2} (Q_{ij}^s - \varepsilon_e^s)^2 \\ &\times \frac{F(Z+1, \varepsilon_e^s)}{1 + \exp[(U_F - \varepsilon_e^s)/k_B T]}. \end{aligned} \quad (14)$$

Therefore, according to Equation (1), the beta decay rate with SES is given by

$$\lambda_{\text{bd}}^s = \ln 2 \sum \frac{(2J_i + 1) e^{\frac{-E_i}{k_B T}}}{G(Z, A, T)} \sum_f \frac{\psi^s(\rho, T, Y_e, Q_{ij}^s)}{ft_{ij}^s}, \quad (15)$$

where the half-life  $ft_{ij}^s$  is defined as

$$\begin{aligned} \ln(ft_{ij}^s) &= a_1 + \left( \alpha^2 Z^2 - 5 + a_2 \frac{N-Z}{A} \right) \\ &\ln(Q_{if}^s - a_3 \delta) + (a_4 \alpha^2 Z^2) \\ &+ \frac{1}{3} \alpha^2 Z^2 \ln(A) - \alpha Z \pi + S(N, Z). \end{aligned} \quad (16)$$

We compare the results ( $\lambda_{\text{bd}}^s$ ) in SES with those of the rates ( $\lambda_{\text{bd}}^0$ ) without SES by defining an enhancement factor  $C$ , which is written as

$$C = \frac{\lambda_{\text{bd}}^s}{\lambda_{\text{bd}}^0}. \quad (17)$$

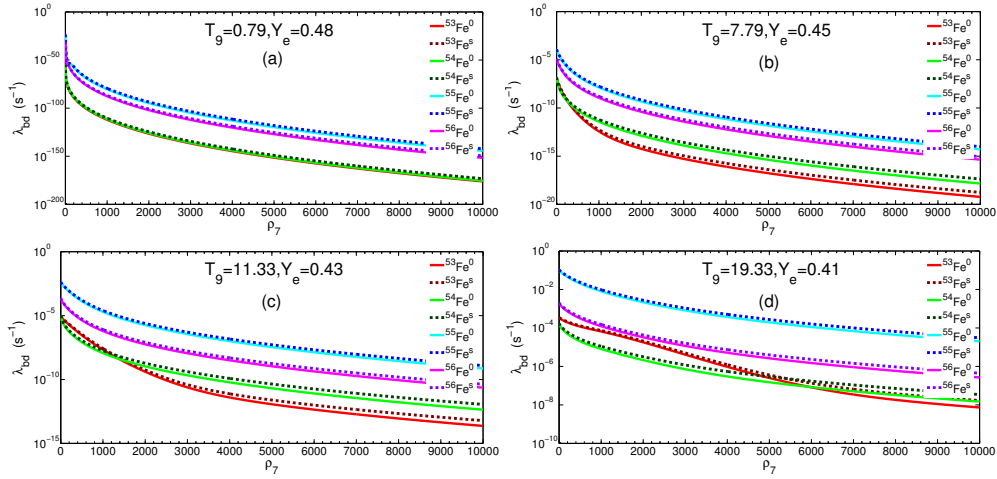
### 3 NUMERICAL RESULTS AND DISCUSSIONS

Based on the proton-neutron quasiparticle random phase approximation (pn-QRPA) model, Nabi (2010) investigated the beta decay rates in supernovae. Under the same conditions, Fuller et al. (1982) and Aufderheide et al. (1990, 1994) also discussed the beta decay rates. Their studies show that the beta decay rates play an important role in core collapse calculations and evolution. However, they neglected the effect of SES on beta decay. Here based on LRTM, we discuss beta decay for SES models (I) and (II). Models (I) and (II) correspond to the cases without and with correction by the  $Q$ -value respectively.

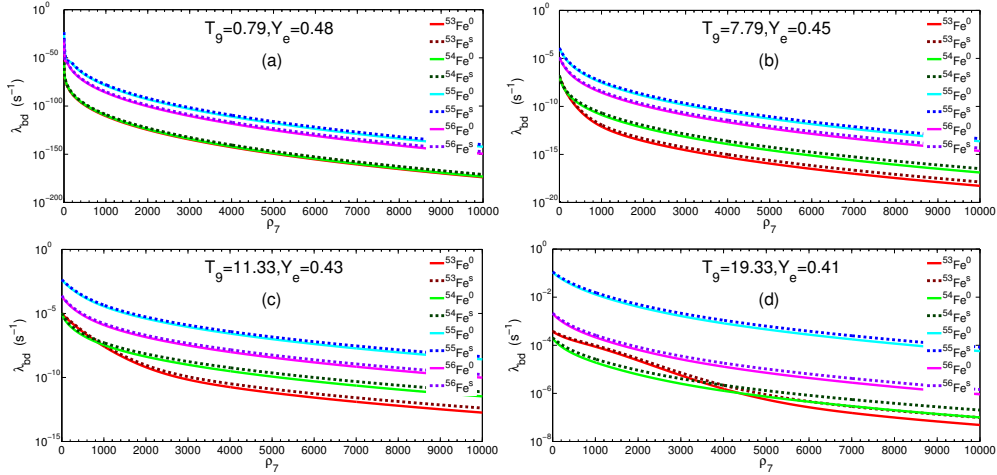
Figures 1 and 2 present the influences of density on beta decay rates of some iron group isotopes for the two SES models. The no SES and SES rates can be compared and correspond to solid and dotted lines respectively. We provide details about the GT transition contribution for beta decay according to the SMMC method. For a given temperature, we find that the beta decay rates decrease by more than six orders of magnitude as the density increases. The strong screening rates are always higher than those without SES. For example, at  $\rho_7 = 5000$ ,  $T_9 = 7.79$ ,  $Y_e = 0.45$  the rates for  $^{53}\text{Fe}$  are  $1.716 \times 10^{-17}$  and  $4.065 \times 10^{-17}$  corresponding to those of no SES and SES for model (I) in Figure 1(b), but are  $1.129 \times 10^{-16}$  respectively, and  $2.451 \times 10^{-16}$  for model (II) in Figure 2(b). The SES beta decay rates of model (II) are more than one order of magnitude higher than those of model (I).

Figure 3 shows the screening enhancement factor  $C$  as a function of  $\rho_7$ . Due to SES, the rates may increase by about two orders of magnitude. For instance, the screening enhancement factor  $C$  increases from 11.55 to 170.8 when the density increases from  $10^3$  to  $10^4$  for  $^{53}\text{Fe}$  at  $T_9 = 0.79$ ,  $Y_e = 0.48$  for model (II) in Figure 3(a). The lower the temperature, the larger the effect of SES on beta decay rates is. One possible cause is that SES mainly increases the number of higher energy electrons. These electrons can actively join in the beta decay reaction. Moreover, SES can also make the beta decay threshold energy greatly decrease. Thus, SES strongly encourages beta decay reactions. One also finds that the values of SES enhancement factor  $C$  for model (II) are higher than those for model (I). For example, at  $\rho_7 = 7000$ ,  $T_9 = 0.79$ ,  $Y_e = 0.48$ , values of the screening factor  $C$  for  $^{53,54,55,56}\text{Fe}$  are 88.09, 86.18, 70.11, 70.53 for model (I) and are 98.36, 95.89, 82.56, 84.12 for model (II), as displayed in Figure 3(a).

Tables 1 and 2 show the screening enhancement factor  $C$  at  $\rho_7 = 1000$  and 10000 respectively for models (I) and (II). From Table 1, the screening rates for



**Fig. 1** The beta decay rates of  $^{53}\text{Fe}$ ,  $^{54}\text{Fe}$ ,  $^{55}\text{Fe}$  and  $^{56}\text{Fe}$  as a function of electron density  $\rho_7$  with (dotted lines) and without (solid lines) SES for model (I).



**Fig. 2** The beta decay rates of  $^{53}\text{Fe}$ ,  $^{54}\text{Fe}$ ,  $^{55}\text{Fe}$  and  $^{56}\text{Fe}$  as a function of electron density  $\rho_7$  with (dotted lines) and without (solid lines) SES for model (II).

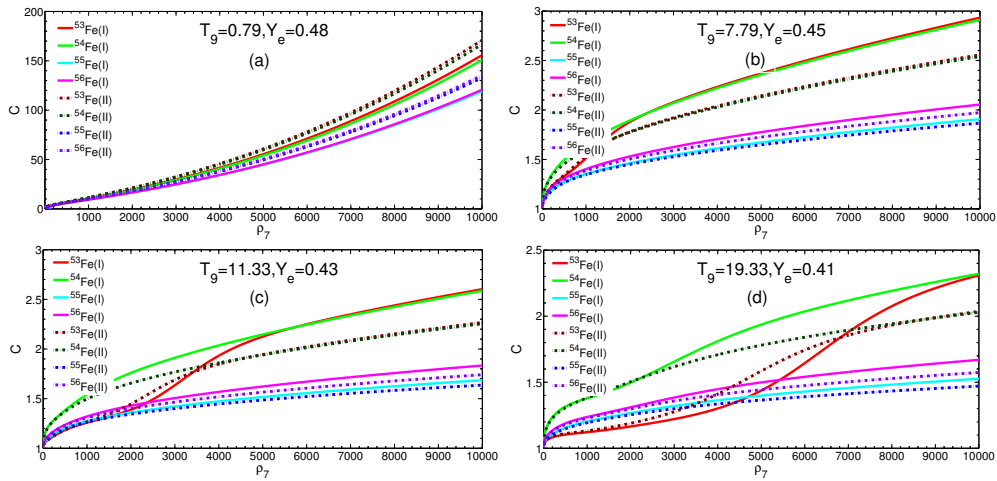


**Fig. 3** The screening enhancement factor  $C$  for beta decay rates of  $^{53}\text{Fe}$ ,  $^{54}\text{Fe}$ ,  $^{55}\text{Fe}$  and  $^{56}\text{Fe}$  as a function of electron density  $\rho_7$  for models (I) and (II).

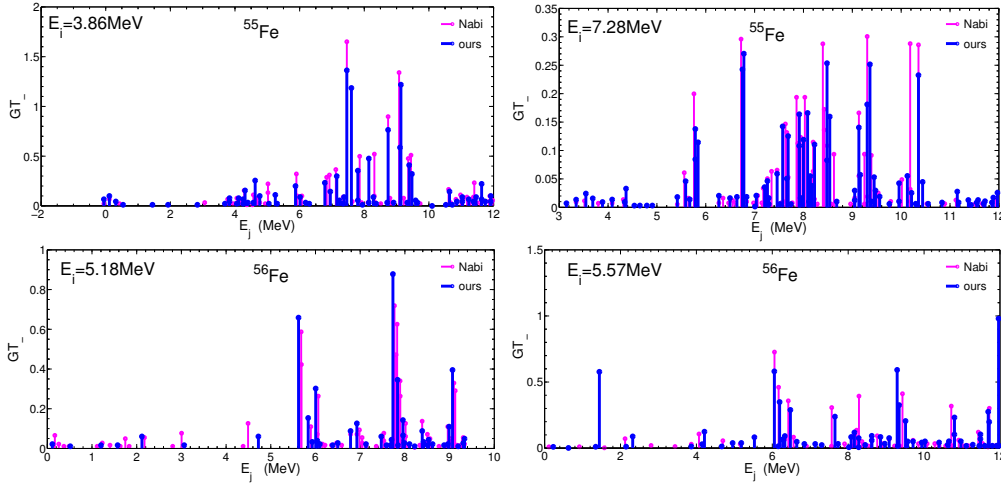


**Fig. 4** Comparisons of the excited state GT strength distributions for  $^{55}\text{Fe}$  and  $^{56}\text{Fe}$  between ours and Nabi.  $E_i(E_j)$  represents parent (daughter) energy states.

**Table 1** The Strong Screening Enhancement Factor  $C$  for Models (I) and (II) at  $\rho_7 = 1000$  in Some Typical Astronomical Conditions

Nuclei	$T_9 = 0.79, Y_e = 0.48$		$T_9 = 7.79, Y_e = 0.45$		$T_9 = 11.33, Y_e = 0.43$		$T_9 = 19.33, Y_e = 0.481$	
	$C(\text{I})$	$C(\text{II})$	$C(\text{I})$	$C(\text{II})$	$C(\text{I})$	$C(\text{II})$	$C(\text{I})$	$C(\text{II})$
$^{53}\text{Fe}$	10.59	11.56	1.523	1.563	2.602	2.266	1.121	1.133
$^{54}\text{Fe}$	10.43	11.46	1.686	1.611	2.584	2.252	1.376	1.377
$^{55}\text{Fe}$	9.288	10.19	1.347	1.353	1.686	1.636	1.203	1.193
$^{56}\text{Fe}$	9.349	10.32	1.415	1.399	1.833	1.741	1.237	1.228

**Table 2** The Strong Screening Enhancement Factor  $C$  for model (I) and (II) at  $\rho_7 = 10000$  in Some Typical Astronomical Conditions

Nuclei	$T_9 = 0.79, Y_e = 0.48$		$T_9 = 7.79, Y_e = 0.45$		$T_9 = 11.33, Y_e = 0.43$		$T_9 = 19.33, Y_e = 0.481$	
	$C(\text{I})$	$C(\text{II})$	$C(\text{I})$	$C(\text{II})$	$C(\text{I})$	$C(\text{II})$	$C(\text{I})$	$C(\text{II})$
$^{53}\text{Fe}$	155.7	170.8	2.931	2.566	1.258	1.267	2.320	2.034
$^{54}\text{Fe}$	150.6	166.7	2.911	2.539	1.542	1.497	2.332	2.028
$^{55}\text{Fe}$	118.9	132.8	1.905	1.866	1.273	1.264	1.526	1.470
$^{56}\text{Fe}$	120.6	135.2	2.055	1.972	1.321	1.306	1.669	1.573

$^{53,54,55,56}\text{Fe}$  increase by factors of 10.59, 10.43, 9.288 and 9.349 at  $\rho_7 = 1000, T_9 = 0.79, Y_e = 0.48$  for model (I) and by factors 11.56, 11.46, 10.19 and 10.32 for model (II). From Table 2, the screening rates for  $^{53,54,55,56}\text{Fe}$  increase by factors of 155.7, 150.6, 118.9 and 120.6 at  $\rho_7 = 10000, T_9 = 0.79, Y_e = 0.48$  for model (I), and by factors of 170.8, 166.4, 132.2 and 135.2 for model (II). However, the difference in screening enhancement factor  $C$  between models (I) and (II) is small at the higher temperature. This is because at the higher temperature, the electron energy is larger for a given density, so the higher temperature weakens the effect of SES on beta decay.

The beta decay rates strongly depend on the decay  $Q$ -value. The higher the energy of an outgoing electron, the larger the rates become when the electron energy is more than the threshold energy. When we account for the  $Q$ -value correction in model (II), according to Equation (4), the half-life will increase as the  $Q$ -value

increases. The nuclear binding energy increases because of interactions with the dense electron gas in the plasma. The beta decay  $Q$ -value ( $Q_{if}$ ) changes at high density due to the effect of charge dependence in this binding. Based on Equation (13), the  $Q$ -value of beta decay decreases from  $Q_{if}$  to  $Q_{if} - \Delta Q$ . Thus, the beta decay will increase due to correction by the  $Q$ -value in model (II) according to Equation (1) and Equation (4).

In supernova evolution the distributions of GT strength for various nuclides play a key role. As examples for the excited state GT distributions of  $^{55,56}\text{Fe}$ , Figure 4 presents some information about the comparison between our results by SMMC and those of Nabi (2010) for beta decay. Only the first two excited state distributions are shown. From Figure 4, one finds that our calculated results of GT strength distributions are lower than those of Nabi. For example, the  $GT^-$  distributions for  $^{55}\text{Fe}$  are 1.650 MeV, 1.362 MeV corresponding to Nabi's and ours at  $E_i = 3.86\text{MeV}, E_j =$

7.461 MeV, and are 0.7265 MeV, 0.5865 MeV for  $^{56}\text{Fe}$  at  $E_i = 5.18$  MeV,  $E_j = 6.055$  MeV respectively. Based on pn-QRPA theory, Nabi (2010) analyzed nuclear excitation energy distribution by considering the particle emission processes. They calculated GT strength distribution and only discussed the low angular momentum states. By using the method of SMMC, actually we discuss GT intensity distribution and adopt an average distribution.

Synthesizing the above analysis, we conclude that charge screening has strong effects on beta decay. The influence may mainly come from the following several factors. First, the electron Coulomb wave function is strongly changed by the screening potential in nuclear reactions. Second, the energy of outgoing electrons increases greatly due to the electron screening potential. Third, the energy of atomic nuclei also increases because of the electron screening (i.e., increases the single particle energy). Finally, the electron screening effectively makes the number of higher-energy electrons increase. So, the electron energy is more than the threshold of beta decay. SES relatively decreases the threshold needed for beta decay.

#### 4 CONCLUDING REMARK

Based on LRTM and Fermi theory, we discuss the beta decay process for two typical SES models (i.e., models (I) and (II)). We detail the GT transition contribution to beta decay according to the SMMC method. For a given temperature, the beta decay rates decrease by more than six orders of magnitude with an increase of density. The strong screening rates are always higher than those of no SES. The SES beta decay rates of model (II) are by more than one order of magnitude higher than those of model (I). Our results show that the beta decay rates increase by about one order of magnitude due to SES. For instance, the screening enhancement factor  $C$  increases from 11.55 to 170.8 when the density increases from  $10^3$  to  $10^4$  for  $^{53}\text{Fe}$  at  $T_9 = 0.79$ ,  $Y_e = 0.48$  for model (II). The beta decay rates and antineutrino energy loss are quite relevant for numerical simulations of stellar thermal evolution. Our results may be helpful to future studies of the burst mechanism of supernovae and related numerical simulations of cooling.

**Acknowledgements** This work was supported in part by the National Natural Science Foundation of China (Grant 11565020), the Counterpart Foundation of Sanya (Grant 2016PT43), the Special Foundation of Science and Technology Cooperation for Advanced Academy and Region of Sanya (Grant 2016YD28), the Scientific Research Starting Foundation for 515 Talented Project of Hainan Tropical Ocean University (Grant

RHDFRC201701) and the Natural Science Foundation of Hainan Province (Grant 114012).

#### References

- Aufderheide, M. B., Brown, G. E., Kuo, T. T. S., Stout, D. B., & Vogel, P. 1990, *ApJ*, 362, 241
- Aufderheide, M. B., Bloom, S. D., Resler, D. A., & Mathews, G. J. 1993, *Phys. Rev. C*, 48, 1677
- Aufderheide, M. B., Fushiki, I., Woosley, S. E., & Hartmann, D. H. 1994, *ApJS*, 91, 389
- Bludman, S. A., & van Riper, K. A. 1978, *ApJ*, 224, 631
- Domingo-Pardo, C., Dillmann, I., Faestermann, T., et al. 2009, in *AIPC Series*, 1090, eds. J. Jolie, A. Zilges, N. Warr, & A. Blazhev, 230
- Fuller, G. M., Fowler, W. A., & Newman, M. J. 1982, *ApJS*, 48, 279
- Gao, Z. F., et al. 2015, *Astron. Nachr.* 336, 866
- Gao, Z. F., et al. 2016, *MNRAS*, 456, 55
- Gao, Z. F., et al. 2017a, *Astron. Nachr.* DOI: 10.1002/asna.201713436; arXiv:1709.02734
- Gao, Z. F. et al. 2017b, *ApJ*, 849, 19
- Gao, Z. F. et al. 2017c, 2017, *Astron. Nachr.* DOI: 10.1002/asna.201713437
- Itoh, N., Tomizawa, N., Tamamura, M., Wanajo, S., & Nozawa, S. 2002, *ApJ*, 579, 380
- Jancovici, B. 1962, *Il Nuovo Cimento*, 25, 428
- Langanke, K., & Martinez-Pinedo, G. 1998, *Physics Letters B*, 436, 19
- Langanke, K., Terasaki, J., Nowacki, F., Dean, D. J., & Nazarewicz, W. 2003, *Phys. Rev. C*, 67, 044314
- Liu, J. J. 2012, *Chinese Physics Letters*, 29, 122301
- Liu, J. J. 2013a, *RAA (Research in Astronomy and Astrophysics)*, 13, 945
- Liu, J. J. 2013b, *Chinese Physics C*, 37, 085101
- Liu, J. J. 2013c, *MNRAS*, 433, 1108
- Liu, J. J. 2013d, *Ap&SS*, 343, 579
- Liu, J. J. 2013e, *Ap&SS*, 343, 117
- Liu, J. J. 2013f, *RAA (Research in Astronomy and Astrophysics)*, 13, 99
- Liu, J. J. 2014, *MNRAS*, 438, 930
- Liu, J. J. 2015, *Ap&SS*, 357, 93
- Liu, J. J. 2016, *RAA (Research in Astronomy and Astrophysics)*, 16, 83
- Liu, J. J., & Gu, W. M. 2016, *ApJS*, 224, 29
- Liu, J. J., Kang, X. P., Hao, L. H., et al. 2016, *RAA (Research in Astronomy and Astrophysics)*, 16, 174
- Liu, J. J., Peng, Q. H., Hao, L. H., Kang, X. P., & Liu, D. M. 2017a, *RAA (Research in Astronomy and Astrophysics)*, 17, 107
- Liu, J. J., Peng, Q. H., & Liu, D. M. 2017b, *Chinese Physics C*, 41, 095101
- Nabi, J. U. 2010, *Advances in Space Research*, 46, 1191
- Zhou, Y., Li, Z., Wang, Y., et al. 2017, *Science China Physics, Mechanics, and Astronomy*, 60, 82012